Available online at www.sciencedirect.com
ScienceDirect
Physics Letters A 370 (2007) 70–77
PHYSICS LETTERS A
www.elsevier.com/locate/pla

Predictions and observations of low-shear beta-induced shear Alfvén–acoustic eigenmodes in toroidal plasmas ☆

N.N. Gorelenkov [a,*], H.L. Berk [b], E. Fredrickson [a], S.E. Sharapov [c], JET EFDA Contributors [1]

[a] *Princeton Plasma Physics Laboratory, Princeton University, USA*
[b] *IFS, Austin, Texas, USA*
[c] *Euroatom/UKAEA Fusion Association, Culham Science Centre, Abingdon, Oxfordshire, USA*

Received 11 April 2007; accepted 9 May 2007

Available online 12 June 2007

Communicated by F. Porcelli

Abstract

New global MHD eigenmode solutions arising in gaps in the low frequency Alfvén–acoustic continuum below the geodesic acoustic mode (GAM) frequency have been found numerically and have been used to explain relatively low frequency experimental signals seen in NSTX and JET tokamaks. These global eigenmodes, referred to here as Beta-induced Alfvén–Acoustic Eigenmodes (BAAE), exist in the low magnetic safety factor region near the extrema of the Alfvén–acoustic continuum. In accordance to the linear dispersion relations, the frequency of these modes shifts as the safety factor, q, decreases. We show that BAAEs can be responsible for observations in JET plasmas at relatively low beta $< 2\%$ as well as in NSTX plasmas at relatively high-beta $> 20\%$. In contrast to the mostly electrostatic character of GAMs the new global modes also contain an electromagnetic (magnetic field line bending) component due to the Alfvén coupling, leading to wave phase velocities along the field line that are large compared to the sonic speed. Qualitative agreement between theoretical predictions and observations are found.

1. Introduction

An area where up to now there has been sporadic investigation [1–6] but where pertinent wave particle interactions in burning plasma regimes need to be investigated, is the theoretical and experimental study of the linear interaction of between shear Alfvén and acoustic waves, two of the fundamental excitations of plasma in MHD theory in toroidal geometry. The interaction is mediated by finite pressure, plasma compressibility and the geodesic curvature. As a result of such interaction additional gaps in the coupled Alfvén–acoustic continuum emerge [6,7] and here we present an analytic model for the structure of these gaps. In addition their Alfvén–acoustic continuum has extrema with respect to the radial position, which arise in the gaps or in the low shear regions. We find with the use of the NOVA code [8] that global modes may occur adjacent to these extrema points, but were not reported before.

We call these new global modes associated with Alfvén–acoustic continuum gaps as the Beta-induced Alfvén–Acoustic Eigenmodes (BAAE) and we find that they can appear in both relatively low and relatively high-beta plasmas. We will present data of hitherto unexplained oscillations in JET (relatively low beta) and NSTX (relatively high-beta) in order to test how well MHD theory might explain these observations. Numerical simulations indicate that there are qualitative tendencies of the data to follow MHD theory, but our study also indicates there is a need of a comprehensive kinetic theory to be developed to accurately explain the data. Present kinetic theories seem to be insufficiently complete for this problem as we discuss in the summary section.

☆ This work supported in part by the US Department of Energy under the contracts DE-AC02-76CH03073 and DE-FG03-96ER-54346 and in part by the European Fusion Development Agreement.
* Corresponding author.
E-mail address: ngorelen@pppl.gov (N.N. Gorelenkov).
[1] See Appendix of M.L. Watkins et al. [M.L. Watkins, et al., Fusion Energy 2006, Proc. 21st Int. Conf. Chengdu, 2006, IAEA, Vienna, 2006].

0375-9601/$ – see front matter
doi:10.1016/j.physleta.2007.05.113

Numerical calculations for monotonic safety factor, q-, profile and observations on JET show that the BAAE modes evolve from zero frequency, when q_0 or $q_{\min}$ cross rational values, and is bounded by a certain maximum value, which is determined by the frequency of the Alfvén–acoustic gap. By understanding the range of BAAE frequency excitation and observing or exciting these frequencies in experiments it seems potentially possible to extend the use of MHD to determine q_0 or $q_{\min}$. Such observations could be a very important diagnostic tool for ITER and other burning plasma experiments. These observations would also help to infer the central plasma beta and the ion and electron temperatures.

In JET observations near the lowest possible frequency of the mode, the wave properties are quite similar to that of a shear Alfvén wave which is characterized by a magnetic field line bending perturbation, but with a dispersion that is modified from the conventional shear Alfvén wave dispersion. We have found qualitative agreement between theoretical predictions and observations, but there is a disparity that remains to be resolved in the quantitative matching of the predicted frequency with experimental observations.

In NSTX with the plasma beta around 20%, the BAAE modes are found numerically using the ideal MHD NOVA code. They are located within the Alfvén–acoustic continuum gaps and these BAAEs match hitherto unexplained oscillations in NSTX. They are localized near the region of low shear in plasmas with a reversed shear profile. In this case the frequency is about half the TAE frequency and is close to the geodesic acoustic mode (GAM) frequency. In NSTX, there is typically a strong drive from beam ions and it appears that the BAAEs contribute to a rather strong fast ion radial redistribution and loss. The frequency of the BAAE modes is in good agreement with that measurements when corrected for the Doppler shift due to the rotation.

The Letter is organized as follows. In Section 2 we derive expression for the Alfvén–acoustic continuum, its extremum points and the frequency gap. We apply our theory to JET and NSTX plasmas in Sections 3 and 4, respectively, where NOVA simulation results are also presented. A summary and a discussion of the relation of our work to previous publications are given in Section 5.

2. Low frequency Alfvén–acoustic continuum

We start from the ideal MHD equations for the continuum, which incorporates both the shear Alfvén and the acoustic branches (neglecting drift effects) [8,9]

$$\omega^2\rho\frac{|\nabla\psi|^2}{B^2}\xi_s + (\mathbf{B}\cdot\nabla)\frac{|\nabla\psi|^2}{B^2}(\mathbf{B}\cdot\nabla)\xi_s + \gamma p k_s \nabla\cdot\vec{\xi} = 0,$$
$$\frac{\gamma p}{B^2} + 1 \quad \nabla\cdot\vec{\xi} + \frac{\gamma p}{\omega^2\rho}(\mathbf{B}\cdot\nabla)\frac{\mathbf{B}\cdot\nabla}{B^2}\nabla\cdot\vec{\xi} + k_s\xi_s = 0, \qquad (1)$$

where ψ is the poloidal magnetic flux, p and ρ are the plasma equilibrium pressure and density, γ is the specific heat ratio, $\xi_s \equiv \vec{\xi}\cdot[\mathbf{B}\times\nabla\psi]/|\nabla\psi|^2$, $\vec{\xi}$ is the plasma displacement, $k_s \equiv 2\mathbf{k}\cdot[\mathbf{B}\times\nabla\psi]/|\nabla\psi|^2$ and $\mathbf{k}$ and $\mathbf{B}$ are vectors of the magnetic curvature and field. The baseline physics of the Alfvén–acoustic mode coupling and the formation of the continuum and global modes in toroidal geometry can be understood in the limit of a low beta, high aspect ratio plasma. Making use of this tokamak ordering we find that the expression for the geodesic curvature is $k_s = 2\varepsilon\sin\theta/q$, where $\varepsilon = r/R \ll 1$ and we neglected corrections of order $O(\varepsilon^2)$ and higher. This is justified for the low mode frequency, such that $\Omega^2 = O(1)$, where we defined $\Omega^2 \equiv (\omega R_0/v_A)^2/\delta$ and $\delta \equiv \gamma\beta/2 = O(\varepsilon^2)$. Thus, keeping only leading order terms we reduce the system of Eqs. (1) to (for details see Ref. [10])

$$\Omega^2 y + \delta^{-1}\partial_\parallel^2 y + 2\sin\theta z = 0, \qquad (2)$$
$$\Omega^2 z + \partial_\parallel^2 z + 2\Omega^2\sin\theta y = 0, \qquad (3)$$

where $y \equiv \xi_s\varepsilon/q$, $z \equiv \nabla\cdot\vec{\xi}$, $\partial_\parallel \equiv R_0 d/dl$ and l is the distance along the field line. For sufficiently small values of ε and β, numerical solutions of Eqs. (1)–(3) are found to be almost identical to numerical solutions of the NOVA code [8], which solves Eqs. (1). For this section, we can then consider Eqs. (1) and (2), (3) to be interchangeable.

Eq. (2) is essentially the shear Alfvén wave equation if z term is neglected. Eq. (3) for z alone, would be the conventional sound equation. The two equations couple due to the finite compressibility of the plasma in toroidal geometry to give the form shown in Eqs. (2), (3). The coupling of each branch with the dominant poloidal mode number m, is via the $m\pm1$ sideband harmonics of the other branch. To treat the side band harmonics we employ the following form for the perturbed quantities

$$\begin{matrix} y \\ z \end{matrix} = \sum_j \begin{matrix} y_{j-m}(r) \\ z_{j-m}(r) \end{matrix} e^{-i\omega t + ij\theta - in\zeta}, \qquad (4)$$

where ζ is the ignorable toroidal angle along the torus, the direction of symmetry.

By substituting Eq. (4) into Eqs. (2), (3) to eliminate $z_{j\pm1}$ in terms of y_j and $y_{j\pm2}$ we find a three term recursion relation

$$\Omega^2 - \frac{k_j^2}{\delta} - \Omega^2\left(\frac{1}{\Omega^2 - k_{j-1}^2} + \frac{1}{\Omega^2 - k_{j+1}^2}\right) y_j + \Omega^2\left(\frac{y_{j-2}}{\Omega^2 - k_{j-1}^2} + \frac{y_{j+2}}{\Omega^2 - k_{j+1}^2}\right) = 0.$$

One can readily justify that for $j = 0$ we can ignore the side band terms in the limit $\delta \ll 1$. Then the coefficient of y_0 must vanish and we obtain the following dispersion relation (similar to Ref. [6])

$$\Omega^2 - k_0^2/\delta \quad \Omega^2 - k_{+1}^2 \quad \Omega^2 - k_{-1}^2 = \Omega^2\ 2\Omega^2 - k_{+1}^2 - k_{-1}^2\ . \qquad (5)$$

The left-hand side set to zero, represents oscillations in an infinite medium, the two acoustic modes $\Omega^2 = k_{\pm1}^2$ and the shear Alfvén wave $\Omega^2 = k_0^2/\delta$, in the absence of toroidal effects and this is valid for $k_0^2/\delta \gg 1$. However the character of the solutions drastically changes for $k_0^2/\delta \ll 1$.

Then as $|k_{\pm1}| \gg |k_0|$ in the vicinity of $q = m/n$ we can approximate $k_j^2 = (j/q + k_0)^2 \simeq j^2/q^2 + 2k_0 j/q$. Note, that in

the high-m, n limit the radial dependence can be kept in the k_0 term only and $q = q_r = m/n$ can be fixed at the rational surface value, that is $k_j^2 \simeq j^2/q_r^2 + 2k_0 j/q_r$. With the coupling effect from the geodesic curvature, we find in the limit $k_0^2/\delta \ll 1$ two low frequency roots. One is

$$\Omega^2 = 1/q^2 \tag{6}$$

(comparable in frequency to the two acoustic side band frequencies), while the second solution takes the form of a modified shear Alfvén wave

$$\Omega^2 = k_0^2/\delta \ 1 + 2q^2 \ . \tag{7}$$

This dispersion also follows from the kinetic theory developed in Ref. [11]. As k_0^2/δ gets larger the modified Alfvén wave frequency, Eq. (7), approaches the frequency of the first solution, Eq. (6), but do not cross. The first solution's frequency, Eq. (6), increases slowly, while the character of the Alfvénic branch solution, Eq. (7), changes dramatically and begins to decrease. As one increases k_0^2/δ further, so that it becomes larger than unity, the larger of the two roots approaches the acoustic side band solution

$$\Omega^2 = k_{\pm 1}^2, \tag{8}$$

taken with plus sign (assuming $k_0 \gg \sqrt{\delta}$ or minus sign if $-k_0 \gg \sqrt{\delta}$) while the smaller of the two solutions (i.e. the modified Alfvén wave, Eq. (7) approaches the other acoustic sideband, Eq. (8), with minus sign (or plus sign if $-k_0 \gg \sqrt{\delta}$). The third root of the dispersion relation given by Eq. (5) in the limit $k_0^2/\delta \ll 1$ is found to be the geodesic acoustic mode (GAM) with a frequency which is larger than the other two modes, i.e. $\Omega^2 = 2(1 + 1/2q^2)$ [12–14]. As k_0^2/δ increases, this mode changes character and becomes the usual shear Alfvén wave $\Omega^2 = k_0^2/\delta$ when $k_0^2/\delta \gg 1$. The same branch was found in Refs. [3] and [2], but was called BAE branch.

As we indicated, when $k_0^2/\delta \sim 1/q^2$ Alfvén and acoustic branches approach each other, but their corresponding roots do not cross. Instead, they form a gap (in frequency) structure that needs to be resolved. Now, we can rewrite Eq. (5) in the following form $4k_0^4/\delta q_r^2 - A^2 k_0^2/\delta + \Omega^2(A-2)A = 0$, where $A = \Omega^2 - q_r^{-2}$. We can solve this equation for $k_0^2(\Omega^2)$ dependence:

$$k_0^2 = \ A^2 \pm \ \sqrt{A^4 - 16\delta\Omega^2 A(A-2)/q_r^2} \ q_r^2/8. \tag{9}$$

This dispersion contains the branches discussed above. We can make use of the properties of Eq. (9) to find the expression for the continuum frequency gap at which $\partial k_0^2/\partial\Omega^2 \to \infty$, that is where k_0^2 has double root. It is easy to see that one of such cases is when $A = 0$, which is found to be a root that corresponds to the upper boundary of the gap, $\Omega = \Omega_+$, where

$$\Omega_+^2 = 1/q_r^2. \tag{10}$$

To find the lower boundary of the gap we consider Eq. (9) together with the double root condition, and find that a cubic equation for A needs to be satisfied: $A^3 - 16\delta(A + q_r^{-2})(A-2)/q_r^2 = 0$ or

$$\hat{A}^3 - (\hat{A} + b)(\hat{A} - d) = 0, \tag{11}$$

where $\hat{A} = q_r^2 A/16\delta$, $b = 1/16\delta$, and $d = 2q_r^2/16\delta$. An exact solution of Eq. (11) can be obtained in general form, but it can be accurately approximated assuming $2q_r^2 > 1$. We find then $\hat{A} = C^{1/3} - d/3C^{1/3}$, where $C = d\sqrt{4d + 27b^2}/6\sqrt{3} - bd/2 > 0$, and the lower boundary gap frequency is expressed by

$$\frac{\Omega_-^2}{\Omega_+^2} = 1 + 16\delta \ \ C^{1/3} - \frac{d}{3C^{1/3}} \ \ . \tag{12}$$

This can be further reduced in the limit of $\delta \ll 1$ to

$$\Omega_-^2 = \Omega_+^2 \ 1 - \ 32q^2\delta \ ^{1/3} \ . \tag{13}$$

However, this last form is accurate only for very low plasma beta, $\delta < 0.2\%$.

Now we compare different continuum solutions obtained here from Eqs. (2), (3), with NOVA solutions obtained from Eqs. (1) for a specific case based on the JET plasma discussed later. In our numerical work the adiabaticity index is taken as $\gamma = 11/8$, which corresponds to equal ion and electron temperatures $T_e = T_i$ in $q \gg 1$ limit [15]. For now we take circular magnetic surfaces with the following plasma parameters: the major radius $R_0 = 2.90$ m, the minor radius $a = 0.0945$ m taken ten times smaller then actual JET plasma radius, plasma beta profile $\beta_{\rm pl} = \beta_{\rm pl0}[1 - (r/a)^5]^2$ (such a beta profile is flat until near the edge and is used in numerical NOVA analyses, but is prescribed exactly flat when we evaluate theoretical equations), $\beta_{\rm pl0} = 0.29\%$, which corresponds to $\delta = 2 \times 10^{-3}$, safety factor profile is taken in the form described in Ref. [9] with a central value $q_0 = 0.99$, edge value $q_1 = 4$, $q' = dq/d\Psi$ equal 0 and 15 at the center and at the edge respectively (it is approximated near the axis as $q \simeq 0.99 + 1.38(r/a)^{4.5}$), where $r/a \equiv \sqrt{\Psi}$ and Ψ is the normalized poloidal flux. The NOVA code numerical solution of Eq. (1) is shown in Fig. 1 to be remarkably close to the analytical solution given by Eq. (9). It is notable that the simplified solutions, Eqs. (7) and (8), are quite close to the numerical solution in the discussed limits $k^2/\delta \ll 1$ (near $r/a = 0.33$) and $k^2/\delta > 1$ (at $r/a > 0.5$).

3. Simulations and observations of BAAEs in low beta JET plasma

It follows from Fig. 1 that the continuum extrema (and potentially global modes) are formed near the magnetic axis, where shear is low, and near gap location, $r/a = 0.45$. We solve ideal MHD equations numerically using NOVA code [8] in JET plasma equilibrium with the parameters given above but with the realistic plasma beta profile $\beta_{\rm pl} = \beta_{\rm pl0}[1 - (r/a)^2]^2\%$, $\beta_{\rm pl0} = 1\%$, central electron density and temperature, $n_{e0} = 1.3 \times 10^{13}$ cm^{-3} and $T_{e0} = 6$ keV, respectively, plasma minor radius $a = 0.95$ m, and last closed magnetic surface ellipticity 1.7 and triangularity 0.23, which together with the q-profile were reconstructed by EFIT code. We fit plasma beta to the

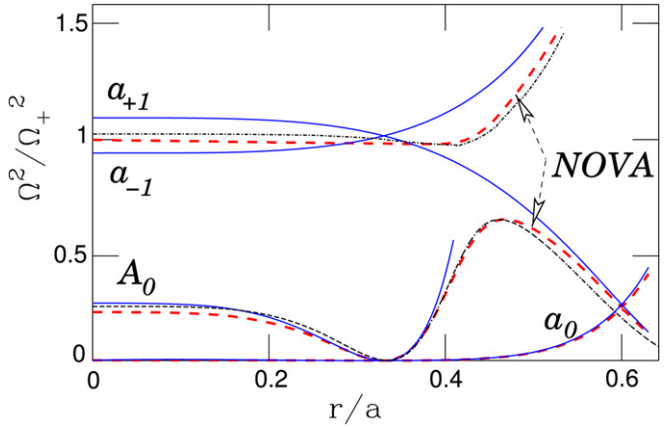

Fig. 1. Comparisons of different approximations for the frequencies of Alfvén–acoustic continuum versus r/a for $\delta = 2 \times 10^{-3}$ shown as red dashed curve (*NOVA*)—the numerical solution of Eq. (1), and black dot-dashed curve—analytical dispersion, Eq. (9). Shown also are "uncoupled" Alfvénic branch, solid curves A_0, corresponding to Eq. (7), sideband ($j = \pm 1$, curves $a_{\pm 1}$) and dominant ($j = 0$, curve a_0) acoustic branches, corresponding to Eq. (8). Frequencies are normalized to Ω_+^2 given by Eq. (10). (For interpretation of the references to colour in this figure legend, the reader is referred to the web version of this Letter.)

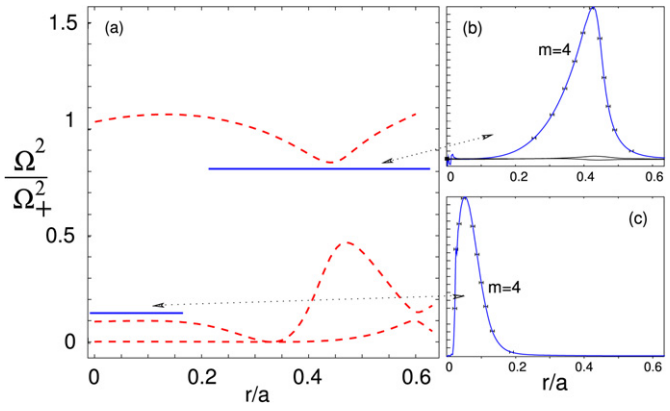

Fig. 2. Alfvén–acoustic continuum (see (a)) is shown as red dashed curves for a JET plasma and $n = 4$, $q_0 = 0.99$. The radial extent of two global BAAEs and their frequencies are shown as solid lines near the extremum points. The radial mode structure of BAAEs located in the gap is shown in (b) as the structure of poloidal harmonics of the normal component of the plasma displacement vector (multiplied by minor radius) in arbitrary units. (c) shows the radial structure of a core localized BAAE. (For interpretation of the references to colour in this figure legend, the reader is referred to the web version of this Letter.)

product of measured electron temperature and density profiles and assumed that $T_i = T_e$, since no measurements of T_i were available at the time of observations. These plasma parameters correspond to the initial (ICRH ramping) phase of JET discharge #62484, in which ~ 2 MW of ICRH power was applied.

In Fig. 2 we show results of NOVA simulations for $n = 4$ and a particular plasma equilibrium with $q_0 = 0.99$, for which we have found two global BAAEs numerically. One mode is localized inside the Alfvén–acoustic gap (Fig. 2(b)), just below the upper boundary of the continuum gap. The second mode is core localized. Its frequency is found just above the modified Alfvén continuum extremum. In this regard core localized BAAE is similar to the up-chirping RSAE [16]. As q_0 decreases in time due to plasma current diffusion, Alfvén–acoustic continuum evolves and so do the frequencies of BAAEs as demonstrated in Fig. 3(a). It is important to note that our theory and numerical simulations predict that core localized BAAE frequency is bounded at high end of its frequency variation by the lower gap frequency, Ω_-, and starts from almost zero value within ideal MHD model. Numerically modes are not found near the lower extremum point inside the gap. This effect may be similar to the TAE frequency downshift due to the pressure gradient (eventually merging into the continuum near the gap at sufficiently strong ∇p) [10,17]. Modes are robustly computed for both flat and slightly reversed q profiles. Reducing plasma density or plasma pressure gradients to zero does not seem to have an effect on BAAE existence or eigenfrequency value. BAAEs normal component of the plasma displacement consist mostly of one poloidal harmonic as can be seen from Fig. 2. However, as expected from our theory, the $m \pm 1$ sidebands of the $\nabla \cdot \vec{\xi}$ perturbation component are also present. It is surprising that the mode width is narrower for the core localized mode, even though the low shear region in the center is wider. It appears that the mode formation mechanisms seem to be different for core-localized (c) and for off-axis (b) modes in Fig. 2.

The measured spectrum of the observed low frequency Mirnov signal in JET discharge #62484 is shown in Fig. 3(b). It contains traces of magnetic signal of several toroidal mode numbers (denoted) from $t \simeq 6.5$ s to $t \simeq 7.1$ s, whose evolution is qualitatively similar to the one obtained in simulations. At this point simple qualitative analysis is sufficient to predict one value of q_0. By comparing Figs. 3(a) and 3(b) we conclude that $q_0 = 1$ at about $t = 6.5$ s, which is consistent with the EFIT equilibrium reconstruction within 3–5% error bars, and the fact that shortly after $t = 7$ s sawteeth-like events were observed on soft X-ray and ECE (electron cyclotron emission) measurements of electron temperature. We note another interesting and unexplained observation, that only even mode numbers were observed $n = -2, 2, 4, 6$, though there are weak $n = 3$ traces in the spectrum.

The toroidal rotation was measured only later in the discharge, but has to be included for the quantitative analysis. It can be evaluated by comparing frequencies of modes with different n numbers, such as $n = -2$ and 2 instabilities at $t = 6.6$ s, i.e. when they have equal frequencies in the lab frame. Assuming that both modes have the same radial location, one can infer the rotation frequency $f_{\rm rot} \simeq 2$ kHz. The same value of $f_{\rm rot}$ follows from the comparison of $n = -2, 2$ and 4 mode frequencies at $t = 7.1$ s, when they can be interpreted as gap modes (pointed by arrows in Fig. 3(b) at $t = 7.1$ s).

However, NOVA simulations predict higher BAAE frequencies. With the assumptions used, $\gamma = 11/8$ (which follows from $T_e = T_i$ [15]) and $\beta_{\rm pl0} = 1\%$ the normalization frequency in Fig. 3(a) corresponds to 51.4 kHz evaluated at $q_r = 1$. Hence, $n = 4$ core localized mode at highest frequency, i.e. $q_0 = 0.96$ (see Fig. 3(a)), has $f \simeq 40$ kHz, which is about three times higher than measured value, $f_{n=4} = 22 - 4 f_{\rm rot} = 14$ kHz. This discrepancy requires further experimental and theoretical studies. One potential way to help to resolve it, is the following. First we note that with the used normalization Fig. 3(a) (as well

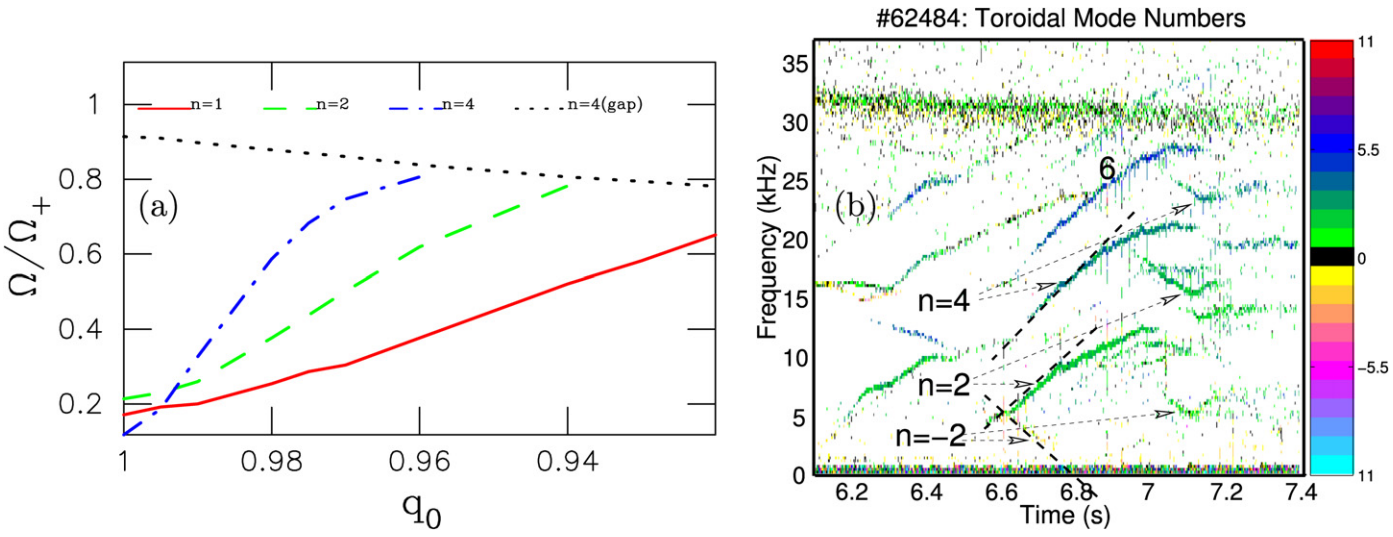

Fig. 3. Several BAAE eigenfrequencies as functions of central safety factor (see (a)). Shown in (a) are core localized mode frequencies for $n = 1$ (solid curve), $n = 2$ (dashed curve), and $n = 4$ (dot-dashed curve) and gap mode frequency for $n = 4$ (dotted curve). Frequencies in (a) are normalized to Ω_+. (b) represents the Mirnov signal frequency spectrum during the start of the discharge #62484. Different colors represent different toroidal mode numbers according to the color chart on the right. Black dashed lines are tangential to the signal initial evolution at $t = 6.6$ s. (For interpretation of the references to colour in this figure legend, the reader is referred to the web version of this Letter.)

as Fig. 2(a)) is not sensitive to the value of γ and plasma beta, which enters through the expression for Ω_+. From our theoretical findings it follows that Ω_+ is lower when electron pressure is larger than the ion pressure. Hence, we should use $\gamma = 1$ and only electron beta for plasma equilibrium, $\beta_{\mathrm{pl}0} = \beta_{e0} = 0.5\%$. This assumption seems to be consistent with the experimental conditions of strong H-minority heating and low plasma density, which means that ICRH power is primarily dumped into the electrons. In this case, we find that Ω_+ corresponds to $f = 31$ kHz, which means that at highest frequency $n = 4$ BAAE has 24.8 kHz. This is 1.77 times larger than the measured value $f_{n=4} = 14$ kHz.

Another effect, which may further reduce the predicted frequency is the reversed safety factor profile, in which case the mode is shifted off-axis, where local plasma pressure can be lower. Since the BAAE frequency depends on the local pressure $\Omega \sim \sqrt{p(r)}$, we expect the frequency to be lower for off-axis BAE localization (i.e. reversed shear). Even though such a frequency downshift is obtained numerically (if correct this result may be useful for tuning up a q-profile reconstruction), the experimental data does not seem to agree with such an assumption as there are observations that the sawtooth inversion radius is close to the plasma center soon after $t = 7.1$ s which then suggests that the q-profile is monotonic.

One plausible reason behind the frequency mismatch is the model for γ, which so far was not properly tested in experiments. It seems possible that a more accurate kinetic treatment is needed. One kinetic effect arising from the ion drift frequency turns out to be negligible. For example for $n = 4$ we find that the drift frequency calculated with the pressure gradient is $\omega_{*pi}/\omega_+ = 1.7 \times 10^{-2}$. Hence, instabilities studied in Refs. [3,11] can not explain the JET observations discussed in this Letter. Finally, energetic particles, which seem to be exciting the BAAE instabilities may cause the shift between the computed and measured mode frequencies [18].

We also note that in the simulations there appears to be a crossing point, where core localized and gap mode frequencies approach each other, such as at $n = 4$ at $q_0 \simeq 0.96$. After this point core localized BAAE disappear due to the interaction with the continuum. Due to the interaction of these two solutions and their different radial localizations, a finite gap in the mode frequencies is expected, which is similar to the TAE/RSAE crossover gaps [19]. This gap in our simulations turns out to be small $< 1\%$ Ω_+, whereas, according to our interpretation, the gap seen in the JET experiments (Fig. 3(b)) is of the order of 10% of the frequency ($n = 4$ mode at $t = 7.1$ s). This may be due to a potentially stronger coupling of the two eigenmodes if kinetic effects are included.

4. Simulations and observations of BAAEs in high-beta NSTX plasma

Our theory predicts that at high plasma beta Alfvén and acoustic modes will be strongly coupled as δ is no longer small. Thus, it is important to investigate predictions of the model and possibly compare with measurements in high-β plasmas, which are typical for spherical tokamaks (ST), such as NSTX. In addition, the safety factor profile measurements with Motion Stark Effect (MSE) diagnostic in NSTX make such study very important for the quantitative validation of the theoretical predictions. We choose NSTX shot #115731, in which previously unexplained MHD activity was observed [20]. The characteristic frequency of such activity is approximately half of the TAE frequency and BAAEs are candidates for the interpretation of these observations.

We take the following plasma parameters $R_0 = 0.806$ m, $a = 0.62$ m, $\beta_{\mathrm{pl}0} = 0.31$, safety factor measured by MSE and shown in Fig. 4(c) has reversed shear region within $r/a \simeq 0.5$, $q_1 \simeq 11$, $q_0 \simeq 2.1$, $q_{\min} = 1.3$, and the same $\gamma = 1.375$ as in previous case, which is consistent with the TRANSP mod-

eling, i.e. $T_i \simeq T_e$. The full MHD continuum spectrum of Eq. (1) is shown in Fig. 4(a) with the radial extent of two found global BAAEs and their frequencies. Frequencies are normalized to Ω_+, which corresponds to 52 kHz. The first radial mode (Fig. 4(b)) has frequency 35 kHz. Again the global BAAE modes are located just above the continuum extremum point in the region of low shear near $q_{\min}$ surface. In this case due to global mode structure of low-n modes (see Figs. 4(b) and 4(c)) and generally strong toroidicity induced coupling of poloidal harmonics in STs, gap BAAE eigenfrequencies are less sensitive to the $q_{\min}$ evolution and are determined by gap envelope extremum rather than by local continuum extremum.

The spectrum of the MHD activity in the NSTX discharge of interest is shown in Fig. 5(a). We plotted the theoretical predictions for the BAAE gap in that figure as a shadowed region. It

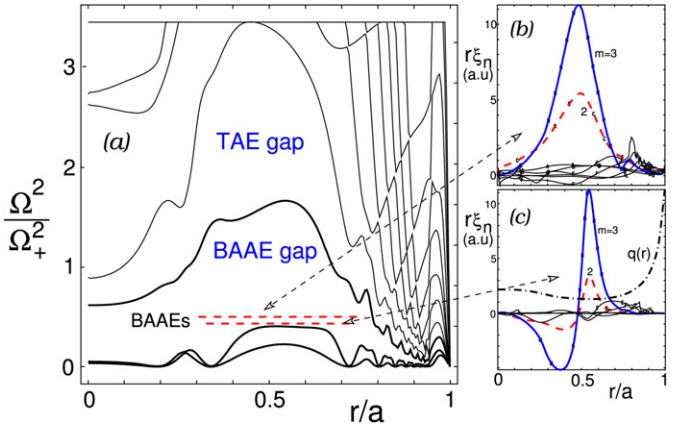

Fig. 4. The same as in Fig. 2(a)–(c), but shown over the whole minor radius and over a wider frequency range, so that both TAE and BAAE gaps are seen as marked. In addition, shown in (c) is the safety factor profile $q(r)$, which is measured by the MSE diagnostic and is reversed at $r/a < 0.6$.

evolves due to the plasma pressure build up in time and due to the plasma spinning up in toroidal direction as the beam ion component increases. Distinct magnetic activity at around $f = 100$ kHz with a toroidal mode number $n = 2$ is seen during the entire discharge. It seems to lie above the approximate TAE frequency curve, but, in fact, such instabilities can be identified as TAE because the TAE gap is wide in NSTX [21]. As the plasma density and pressure increase, the instability frequency moves from TAE frequency range down into the BAAE gap. This is very similar to earlier observations of what was reported as BAEs (beta-induced Alfvén eigenmodes) [22,23], when increasing fast ion and plasma beta resulted in a mode frequency downshift from the TAE frequency into the BAAE frequency range. The same qualitative behavior of instability transition from TAE to a lower frequency was found in kinetic theory [24], but was called there a resonant TAE (rTAE). Note, that the drive of BAAEs in NSTX is expected to be strong due to the beam ion beta being comparable to the thermal ion beta, conditions typical for the NSTX plasma. Fig. 4(a) indicates that the BAAE gap is so wide that during a BAAE burst the mode can stay within the gap even when there is a large frequency variation.

The neutron signal drops at almost each of the BAAE bursts by as much as 8%. In NSTX conditions with large beam ion orbits, this implies that there are strong redistribution and losses of beam ions. The strongest drops in neutron flux coincide with simultaneous bursts of $n = 1$ and $n = 2$ BAAEs, such as at $t = 0.24$ s and $t = 0.255$ s (see Fig. 5(a)). Earlier beam ion losses in NSTX [25] were reported as due to EPMs, which are excited in the same frequency range as BAAEs.

The parameters of the plasma analyzed above correspond to $t = 0.262$ s, when the $n = 2$ magnetic signal activity was measured (pink signal traces as marked). This mode chirps in

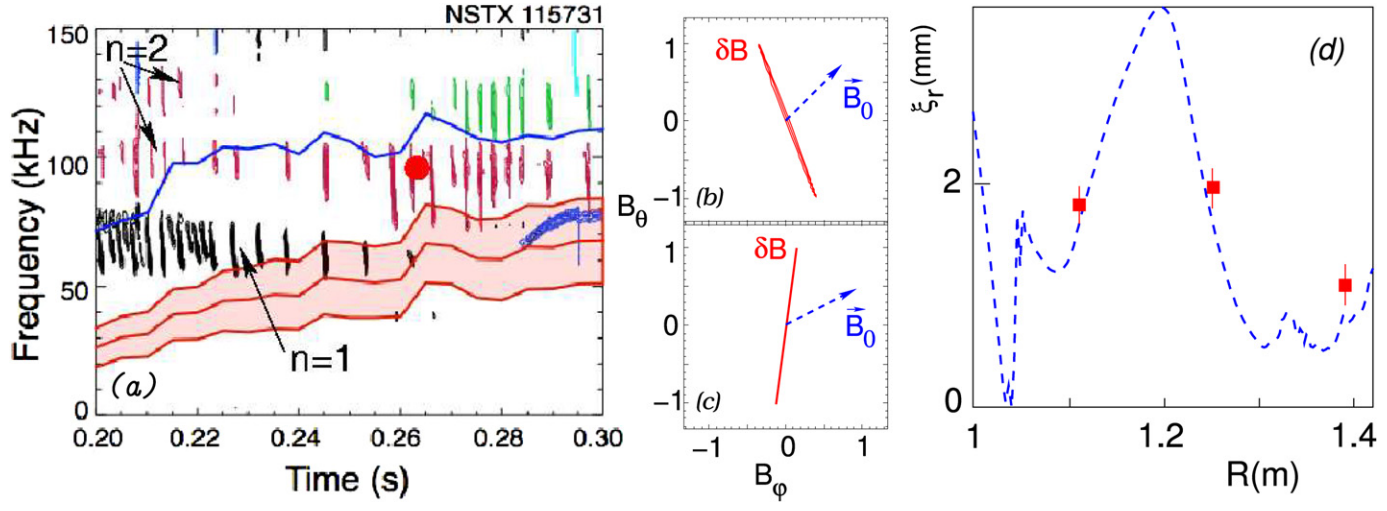

Fig. 5. Magnetic signal spectrum measured at the edge of the plasma in NSTX (see (a)). Shown in (a) are theoretical predictions for the Alfvén–acoustic continuum gap (shaded area between Ω_- and Ω_+) and TAE frequency (separate solid curve corresponding to simple expression $\omega_{\rm TAE} = v_A/qR_0$) for $n = 2$ with the Doppler shift from the plasma rotation contribution included. Red circle point is NOVA predictions for the BAAE frequency. Shown in (b), (c) are the perturbed magnetic field, δB, polarization measured at the edge of the plasma (see (b)) and predicted by NOVA at the peak of the mode amplitude (see (c)), with regard to the equilibrium field, B_0. δB curve traces the tip of its unity vector positioned at the origin of the graphs. (d) shows how NOVA predictions (blue dashed curve) for BAAE radial structure of the radial plasma displacement compares with the reflectometer measurements available at three radial points (marked with red dots). (For interpretation of the references to colour in this figure legend, the reader is referred to the web version of this Letter.)

frequency on a short time scale, typically for a few milliseconds. At the start of the chirp the frequency of the chirping signal in the lab frame is $f_{\rm lab} = 103$ kHz and, if corrected for the measured strong toroidal rotation, $f_{\rm rot} = 30$ kHz (measured by impurities toroidal rotation), gives $f \simeq f_{\rm lab} - n \times 30 = 43$ kHz in the plasma frame. We identify this part of the frequency spectrum (as well as $n = 1$ similar activity shown as black chirping signals) as instability of the BAAE mode because of the following experimental indications. First of all, its frequency within the experimental uncertainties is sufficiently close to the frequency obtained in the simulations. NOVA simulated frequency is shown in Fig. 5(a) as a red circle point, which corresponds to Fig. 5(b) BAAE solution. TAEs were found numerically within TAE gap (see Fig. 4(a)) with the frequency in this case at about 90 kHz in the plasma frame, which means that TAEs can be excluded as candidates in the interpretation of this activity at $t = 0.262$ s, but could be responsible for $n = 2$ oscillations at higher frequency, seen at $f_{\rm lab} = 130$ kHz.

We simulate BAAE polarization with NOVA (Fig. 5(b)) and compare it with measurements (Fig. 5(c)). The polarization is measured only at the edge, whereas NOVA can reliably (within MHD model) predict its polarization only in the eigenmode localization region as the propagation of the mode through the continuum to the edge is not treated self-consistently within the MHD theory. One can see that both numerics and measurements show similar perturbed magnetic field polarizations with regard to the equilibrium magnetic field. In particular, both have strong parallel perturbed field components. However since beta is large in NSTX similar parallel field component of the perturbed field can be expected for Alfvén eigenmodes.

Finally, reflectometer diagnostic provides three radial points of plasma displacement filtered for the one frequency chirp. They can be fitted to the radial displacement structure as show in Fig. 5(d). The radial displacement corresponds to the first radial mode shown in Fig. 4(b).

5. Summary and discussion

In this Letter we have developed a theoretical description of the ideal MHD Alfvén–acoustic continuum gap in the limit of low beta and high aspect ratio plasma. Numerically we have found new global eigenmodes, called here BAAEs, near the extrema points of the continuum in both low and high-beta plasmas. We also presented experimental observations, which support qualitatively and in some cases quantitatively our theoretical predictions. Notably, ideal MHD simulated BAAE frequency evolution qualitatively agrees with JET observations in a low beta plasma, whereas it is quantitatively higher by a factor of 1.77 at the highest frequency predicted for these modes. This is the lowest value ideal MHD can provide by keeping only thermal electron (neglecting bulk ion) pressure. The value of γ as well as kinetic effects such as due to thermal ion FLR and non-perturbative interaction with energetic particles may be responsible for the mismatch in computed and measured mode frequencies [18]. Another potential way to reconcile simulations and observation in JET is to assume that $q_0 = 1.5$, in which case BAAEs with only even toroidal mode numbers can exist and the highest eigenmode frequency will be at 1.5 time lower in simulations. This would bring the NOVA predictions for the BAAE frequency to the value within the experimental uncertainty of 10%. Empirically q_0 seems to be close to unity and measurements of q-profile are required in order to resolve this issue.

In NSTX we found that in the flattop of the discharge the plasma pressure measurement gives several indications that the low frequency oscillations can be identified as BAAE modes. Frequency, mode structure and the polarization data agree with the theoretical predictions within the numerical uncertainty. However, BAAE frequency does not agree with the measurements at the beginning of the discharge as the observed frequency seems to be inside the TAE gap, which is approximately two times the frequency of the BAAE gap in NSTX. This is consistent with the resonant TAE excitation theory in which TAE mode down-shifts and transforms into a BAAE frequency range due to strong drive from fast ions [18,24]. A strong drive is required in NSTX where electron and ion temperatures are similar so that strong ion Landau damping is expected.

However, the problem of BAAE stability is beyond the scope of this Letter. At this stage the question arises on how eigenmodes can exist since the coupling to acoustic branch can result in strong ion Landau damping as the phase velocity of the acoustic branch can be close to the bulk ion thermal velocity. On the other hand even modified Alfvén component of the BAAE, which is clearly electromagnetic, and has phase velocity on the order of Alfvén velocity, can efficiently interact with thermal ions if bulk ion temperature is sufficiently close to the electron temperature. The interaction is due to the poloidal modulation of ion drift velocity resulting in the following transit resonance $\omega - (k_\| \pm 1/qR)v_\| = 0$, which means that since $k_\| \ll 1/qR$ for modified Alfvén wave, thermal ions with $v_\| = v_A k_\| qR = v_{Ti} k_\| qR/\sqrt{\beta_i}$ can efficiently interact with electromagnetic BAAE component. Arguably high ion Landau damping (thus requiring a large drive for instability) means that BAAEs may require non-perturbative studies, such as proposed in Refs. [18,24]. We will address kinetic aspects of BAAE excitation in future publications.

As we mentioned, Alfvén–acoustic continuum was studied in previous publications with the expressions for GAM (or BAE) branches obtained in [2,3,12–14]. Kinetic theory of Ref. [3] does not seem to include acoustic sideband harmonic coupling, so that BAAE gap frequencies were not reported. Expression for the Alfvén–acoustic continuum at the rational surface was found in Ref. [6], whereas numerically BAAE gap structure is shown in Ref. [7]. Global modes corresponding to GAM frequency and called BAE were found in Refs. [23] and [7]. It is clear that the antenna version of the code of Ref. [7] picked up the global mode, which had a strong interaction with the continuum and the eigenfrequency, which is close to the GAM (BAE). More localized global BAAEs with the frequencies below the GAM frequency were not seen in the plasma response. BAAE gap frequency ratio to GAM frequency is $1/\sqrt{2(q^2+1)}$, but both scale the same way with regard to the plasma parameters. However, the frequency evolution of BAAE

(especially the one at the low shear or core region) is notably different from that expected for the GAM (BAE) frequency. Finally, the GAM (BAE) frequency is substantially higher than the BAAE frequency obtained in our work.

Our BAAE based interpretation of JET and NSTX observations is apparently different from the interpretation of low frequency activity in DIII-D [22], which are based on BAE simulations described in Ref. [23]. In that reference BAEs, which matched the measured frequencies, were obtained numerically by explicitly neglecting the acoustic wave coupling. This procedure did not provide any reasonable and physical mode structures in the NOVA simulations of both JET and NSTX plasmas considered due to the strong interaction with the continuum.

The use of BAAE measurements, as we have shown in the example of a JET plasma simulations, can potentially extend the MHD spectroscopy to determine q_0. Such observations could be a very important diagnostic tool for ITER and other burning plasma experiments. These observations would also help to infer the central plasma beta and the ion and electron temperatures by reconciling the measurements and the theory.

Acknowledgements

Supported by DOE contracts Nos. DE-AC02-76CH03073 and DE-FG03-96ER-54346.

References

[1] J.P. Goedbloed, Phys. Fluids 18 (1975) 1258.
[2] M.S. Chu, J.M. Greene, L.L. Lao, A.D. Turnbull, M.S. Chance, Phys. Fluids B 11 (1992) 3713.
[3] F. Zonca, L. Chen, R. Santoro, Plasma Phys. Contr. Fusion 38 (1996) 2011.
[4] J.P. Goedbloed, Phys. Plasmas 5 (1998) 3143.
[5] A.B. Mikhailovskii, S.E. Sharapov, Plasma Phys. Rep. 25 (1999) 803.
[6] B. van der Holst, A.J.C. Beliën, J.P. Goedbloed, Phys. Plasmas 7 (2000) 4208.
[7] G.T.A. Huysmans, W. Kerner, D. Borba, H.A. Holties, J.P. Goedbloed, Phys. Plasmas 2 (1995) 1605.
[8] C.Z. Cheng, M.S. Chance, Phys. Fluids 29 (1986) 3695.
[9] C.Z. Cheng, Phys. Rep. 211 (1992) 1.
[10] N. Gorelenkov, G. Kramer, R. Nazikian, Plasma Phys. Contr. Fusion 48 (2006) 1255.
[11] A.B. Mikhailovskii, S.E. Sharapov, Plasma Phys. Rep. 25 (1999) 838.
[12] N. Winsor, J.L. Johnson, J.M. Dawson, Phys. Fluids 11 (1968) 2448.
[13] B.N. Breizman, S.E. Sharapov, M.S. Pekker, Phys. Plasmas 12 (2005) 112506.
[14] H.L. Berk, C.J. Boswell, D.N. Borba, A.C.A. Figueiredo, T. Johnson, M.F.F. Nave, S.D. Pinches, S.E. Sharapov, Nucl. Fusion 46 (2006) S888.
[15] V.A. Mazur, A.B. Mikhailovskii, Nucl. Fusion 17 (1977) 193.
[16] S.E. Sharapov, B. Alper, H.L. Berk, D.N. Borba, et al., Phys. Plasmas 9 (2002) 2027.
[17] G.Y. Fu, H.L. Berk, Phys. Plasmas 13 (2006) 052502.
[18] N.N. Gorelenkov, W.W. Heidbrink, Nucl. Fusion 42 (2002) 150.
[19] M.A.V. Zeeland, G.J. Kramer, M.E. Austin, R.L. Boivin, W.W. Heidbrin, M.A. Makowski, G.R. McKee, R. Nazikian, W.M. Solomon, G. Wang, Phys. Rev. Lett. 97 (2006) 135001.
[20] N.N. Gorelenkov, H.L. Berk, E.D. Fredrickson, Bull. Am. Soc. 51 (2006) 183.
[21] N.N. Gorelenkov, E. Belova, H.L. Berk, C.Z. Cheng, E.D. Fredrickson, W.W. Heidbrink, S. Kaye, G.J. Kramer, Phys. Plasmas 11 (2004) 2586.
[22] W.W. Heidbrink, E.J. Strait, M.S. Chu, A.D. Turnbull, Phys. Rev. Lett. 71 (1993) 855.
[23] A.D. Turnbull, E.J. Strait, W.W. Heidbrink, M.S. Chu, H.H. Duong, J.M. Greene, L.L. Lao, T.S. Taylor, S.J. Thompson, Phys. Fluids B 5 (1993) 2546.
[24] C.Z. Cheng, N.N. Gorelenkov, C.T. Hsu, Nucl. Fusion 35 (1995) 1639.
[25] E.D. Fredrickson, C.Z. Cheng, D. Darrow, G. Fu, N.N. Gorelenkov, G. Kramer, S.S. Medley, J. Menard, L. Roquemore, D. Stutman, et al., Phys. Plasmas 10 (2003) 2852.